

BL25SU (Soft X-ray Spectroscopy of Solid)

1. Introduction

BL25SU is dedicated to soft X-ray spectroscopic studies on the electronic and magnetic states and the surface structure of solids. After a major upgrade in FY2014, the beamline has two branch lines. The A-branch supports high-energy resolution measurements, while the B-branch is optimized for nano-focused beams with a small angle divergence ^[1-3]. The present status of the main beamline components is described below.

2. Status of the beamline and experimental apparatuses

2-1. Beamline

X-ray intensities at several points in the beamline are regularly monitored to evaluate the condition of the beamline optics since the upgrade in FY2014. In the first year after the upgrade, the photon flux significantly decreased in the A-branch, especially at the carbon absorption edge (~280 eV). The flux decrease is caused by carbon contamination in the reflection surfaces of the pre-focusing mirrors and the diffraction grating. To solve this problem, we studied a new method to reduce the contamination. Clean Si/SiO₂ shrouds can effectively slow the production rate of carbon contamination ^[4]. This indicates that the scattered electrons from the optical element do not generate carbon compounds on the surface of the mirrors and gratings by sputtering the Si/SiO₂ surface, suggesting that the carbon compounds may come from the metallic parts used inside the vacuum chamber. We, therefore, plan to install the same type of the Si/SiO₂ shroud into the beamline optics

in the B-branch after re-cleaning the optical elements. A new varied-line-spacing plane grating with a grooving density of 300 line/mm will be installed in FY2019.

2-2. Two-dimensional photoelectron spectroscopy (A-branch first station)

The apparatus has an analyzer, which can measure the wide-angle distribution of photoelectrons. Using this apparatus, unique methods such as surface-sensitive photoelectron holography ^[5], atomic orbital analysis by circularly polarized resonance photoelectron diffraction ^[6], and microscopic photoelectron diffraction ^[7] have been developed. Due to continuous maintenance, the apparatus is stably operating.

2-3. Retarding field analyzer (RFA) (A-branch second station)

Photoelectron diffraction (PED) or photoelectron holography makes it possible to study non-periodic local structures with multiple chemical states ^[8]. These techniques require wide-range photoelectron angular distribution patterns measured with an energy resolution high enough to resolve core level chemical shifts. Display-type RFAs can observe photoelectron angular distribution patterns with wide acceptance angles ^[9]. However, typical energy resolving power ($E/\Delta E$) of conventional RFAs was ~100, which was insufficient for chemical-state-resolved PED. We developed a new high-resolution display-type RFA ^[10] and achieved $E/\Delta E$ of 1100 with an acceptance angle of $\pm 49^\circ$. In FY2018, we constructed an end station equipped

with the RFA at the A-branch (Fig. 1) and opened it to public users.

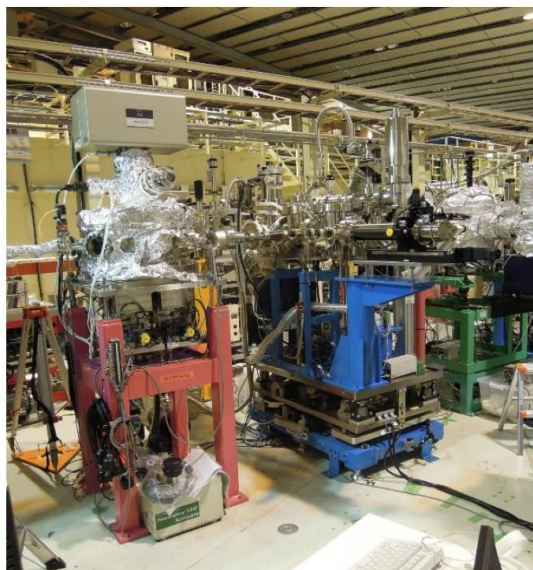


Fig. 1. RFA station constructed at the A-branch of BL25SU.

2-4. Microbeam angle-resolved photoemission spectroscopy (ARPES) (A-branch third station)

The capability of selecting flatly cleaved areas out of poorly cleaved sample surfaces is valuable for ARPES [11]. To enhance this capability, we developed a micro-ARPES system equipped with a DA30 analyzer of Scienta Omicron and a microfocusing mirror [12]. The grazing incidence of soft X-rays onto a sample surface can enhance the photoemission intensity [13]. Thus, we have employed a grazing incidence configuration. This implementation increased the photoemission efficiency more than ten times compared to our previous system. Even with a glancing angle of 5° , the smallest beam spot on a sample, which still has a photon flux tolerable for ARPES, is almost round with an FWHM of $\sim 5 \mu\text{m}$. A spot size of $\sim 10 \mu\text{m}$ on a sample is typically used. This end station (Fig.

2) was installed at the A-branch in January 2018 and opened to public users in April 2018.



Fig. 2. Micro-ARPES station constructed at the A-branch of BL25SU.

2-5. Pulse magnet-type XMCD (B-branch first station)

In an experiment using the pulse magnet-type XMCD apparatus, a long interval time of about 20 min is required to generate 40 T in order to cool down the pulse magnet after each pulse generation. An X-ray shutter linked to the measurement system was installed to avoid unnecessary X-ray irradiation, which causes sample damage. In FY2018, the X-ray shutter system was modified so that it can be controlled by LabVIEW software for stable operations.

2-6. Electromagnet-type XMCD (B-branch second station)

This apparatus can selectively use low temperature, high temperature, and voltage/current application measurements. The combination of these methods

with the total electron yield (TEY), partial fluorescence yield (PFY), and transmission mode can realize a wide variety of experimental environments. To measure samples with a few μm size, we recently updated the manipulator with high-accuracy positioning encoders.

2-7. Scanning soft X-ray microscope (nano-XMCD) (B-branch third station)

The scanning soft X-ray microscope was developed with the support of the Elements Strategy Initiative Center for Magnetic Materials (ESICMM) funded by the Ministry of Education, Culture, Sports, Science and Technology (MEXT) of Japan [14]. This apparatus is unique and features nanoscale MCD imaging under high magnetic fields. It is intensively used to study permanent magnets, where the magnetic field dependent change in the magnetic domains clearly visualizes the microscopic origin of the demagnetization process [15]. In FY2018, the superconducting magnet was updated to a new cryogen-free type, which is manufactured by Cryogenic. Compared to the previous superconducting magnet, the stable range of the magnetic fields (8 T) is twice as wide. The estimated maximum ramping rate of the magnetic fields is 0.53 T/min. Software to measure the magnetic field dependence of the magnetic domains was upgraded so that a sequential measurement is possible when using a table listing the values of magnetic fields at which magnetic images should be measured. We are developing a new sample stage system for temperature dependent experiments.



Fig. 3. New superconducting magnet for nano-XMCD at the B-branch of BL25SU.

Tetsuya Nakamura^{*1}, Takayuki Muro^{*1}, Takuo Ohkochi^{*1}, Yoshinori Kotani^{*1}, Haruhiko Ohashi^{*2}, and Yasunori Senba^{*2}

^{*1} Spectroscopic Analysis Group II, Spectroscopy and Imaging Division, Center for Synchrotron Radiation Research, JASRI

^{*2} Optics and Transport Channel Group, Light Source Division, Center for Synchrotron Radiation Research, JASRI

References:

- [1] T. Nakamura et al., *SPring-8 INFORMATION*, 19, 102-105 (2014).
- [2] T. Nakamura et al., *SPring-8/SACLA Research Report*, 3(1), 186-200 (2015).
- [3] Y. Senba et al., *AIP Conference Proceedings*, 1741, 030044 (2016).
- [4] H. Ohashi et al., *Rev. Sci. Instrum.* **90**, 021704 (2019).
- [5] F. Matsui et al., *Sci. Rep.* **6**, 36258 (2016).
- [6] F. Matsui et al., *Phys. Rev. Lett.* **114**, 011501 (2015).
- [7] K. Sugita et al., *e-J. Surf. Sci. Nanotechnol.* **14**, 59 (2016).
- [8] K. Tsutsui et al., *Nano Lett.* **17**, 7533 (2017).

- [9] S. Kanayama et al., *Rev. Sci. Instrum.* **60**, 2231 (1989).
- [10] T. Muro et al, *Rev. Sci. Instrum.* **88**, 123106 (2017).
- [11] H. Fujiwara et al., *J. Synchrotron Rad.* **22**, 776 (2015).
- [12] Y. Senba et al., *SRI 2018*.
- [13] V. N. Strocov, *J. Synchrotron Rad.* **20**, 517 (2013).
- [14] Y. Kotani et al., *J. Synchrotron Rad.* **25**, 1444-1449 (2018).
- [15] D. Billington et al., *Phys. Rev. Materials* **2**, 104413 (2018).